

# On-ground Testing of a Laminar Flow Wing Leading Edge

O. Steffen, M. Buggisch, J. Kosmann, E. Kappel, H. Köke, C. Hühne  
German Aerospace Center, DLR e.V., Institute of Composite Structures and Adaptive  
Systems, Lilienthalplatz 7, 38108 Braunschweig, Germany

## Abstract

Natural laminar flow on surface areas of transport aircraft is seen as an important contribution to reduction of air travel's CO<sub>2</sub> emissions. Through the course of several national and EU-funded projects, a multi-material leading edge concept was developed and built by the German Aerospace Center, DLR. To validate the design and to demonstrate operational applicability of the leading edge and its specialized NLF compatible attachment concept, a test stand was designed. Capable of deforming a 2.3m Ground Based Demonstrator outer wing section to different surface deformation states, this test stand enables the analysis of the leading edge joint with the upper wing cover and the achieved aerodynamic step height under cruise deformations. It also enables the demonstration of the replacement of a damaged leading edge on a flexible wing on ground.

## 1. INTRODUCTION

Ecological factors, climate change, and economic factors demand for a cut in aircraft fuel consumption to reduce CO<sub>2</sub> emission and aircraft operating cost. A long discussed proposal is to implement areas of prolonged laminar flow on surfaces of transport aircraft. With a contribution of about 18 % to the total friction drag of a typical transport aircraft [1], the wing is exceptionally suited to apply laminar flow technologies. The reduced friction drag of a natural laminar flow wing can lead to a reduction in fuel consumption and thus reduction of CO<sub>2</sub> emissions by up to 8% [2]. However, the laminar boundary layer is sensitive to surface disturbances. Steps, gaps and surface waviness as well as 3D disturbances, such as fastener heads, can trigger early laminar/turbulent transition [3].

To address those challenges, a novel wing leading edge design was conceived at the German Aerospace Center (DLR), initially described in [4]. The implementation and demonstration is part of the Clean Sky 2 effort under the Airframe ITD NACOR proposal.

The overall objective of the project is to demonstrate the eligibility of NLF wing leading edges for real world scenarios and operation. Two major capabilities will be demonstrated:

1. Interchangeability of a full-scale wing leading edge section under operational conditions of a flexible wing
2. Compliance with aerodynamic NLF requirements at the leading edge/wing upper cover joint under cruise deformation.

For validation of the concepts, a 2.3m span ground based demonstrator (GBD) with wing cover and leading edge is built and integrated with the test stand. Different leading edges will be installed, the demonstrator deformed and the surface 3D scanned under cruise deformation.

To achieve this, two interlinked major work packages are being pursued: the detailed design of a leading edge and leading edge attachment as well as its associated manufacturing process and the development of a test stand to enable testing of the leading edge under realistic deformations in a laboratory environment. To validate the

demonstration goals, the test stand will be used to deform the structure to the on-ground and cruise flight surface deformations, where the surface will be 3D scanned and the step between leading edge and wing cover analyzed. In addition, leading edge interchange trials will be done at free-cantilevered wing-on-ground deformation of the demonstrator to show step height compliance with NLF step requirements at operational conditions

## 2. LEADING EDGE CONCEPT

The development of the multi-material laminar wing leading edge and attachment concept is strongly driven by operational requirements. Aerodynamic requirements translate to the following top level design goals for the leading edge attachment:

- Eliminate fastener heads on the outer surface of the wing
- Avoid surface waviness
- Minimize step height between leading edge and wing cover at the respective joint.

From the operational requirements, the following design goals are derived:

- Interchangeability of the leading edge within one night shift
- Enable installation of the leading edge to a deformed wing without rigging → airport apron repair scenario
- Integrate erosion protection
- Keep a minimum structure thickness of 5mm for bird-strike scenarios
- Consideration of systems, such as ice protection, as inert stand-ins

The leading edge is designed as a multi-material composite structure with an integrally bonded steel foil erosion shielding. The requirement for being capable of anti-icing is addressed by the conceptual inclusion of an electro-thermal wing ice protection system (WIPS) consisting of a carbon composite layer isolated with GFRP directly under the erosion shield. Within NACOR, the WIPS is only considered as part of the leading edge's overall composite layout. A functional integration is out-of-scope.

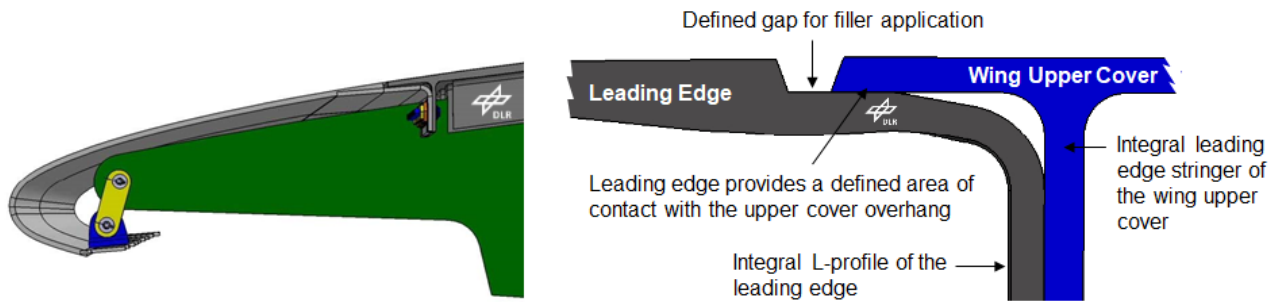


FIGURE 1. Principal arrangement of the leading edge attachment (left) with a strut (yellow) connecting the Krueger flap landing area of the leading edge to the rib and the joint between leading edge and wing upper cover (detailed on the right).

Caused by the asymmetric application (w.r.t. the one-sided WIPS and erosion shield application) of the erosion shielding's steel foil on the leading edge's surface and the mismatch of the coefficients of thermal expansion of CFRP, steel and WIPS structure, variations in temperature lead to shape changes of the leading edge. To compensate for the thermal deformation in operation, the leading edge attachment is designed to be of a pendulum strut-like type (FIG.1, left) with a support free skin from wing cover joint to tip. A conventional attachment with a leading edge fastened chordwise to each leading edge rib, either by fasteners through the outer surface (which would additionally put fastener heads as 3D disturbance on the surface) or by integrated attachment elements on the inside, would lead to local waviness on the surface with changing temperatures. This would not only disturb NLF, but render a global compensation of process induced deformations in the leading edge's production process impossible. The leading edge is joined to the wing box on the inside of the structure to avoid fastener heads on the outer surface. For this purpose, an integral lap joint is created, where the CFRP layup of the leading edge runs under the wing upper cover skin. The joint itself is established between a wing upper cover stringer and an L-shaped extension of the leading edge (FIG. 1, right). Compliance to the laminar flow step height requirements between leading edge and wing cover is ensured by form fit of both parts by the use of fitted fastener elements that prevent any change in the step.

A high degree of part accuracy achieved by the selection of suitable production processes provides a stable mould line at the joint. Thus, material thickness variations otherwise typical to composites have no influence on the joint's step height.

To ensure both the close fit of the leading edge and the wing cover to provide an NLF compatible step and to enable short interchange cycle times in cases where a leading edge has to be replaced, the fasteners at the leading edge joint to the wing cover are combined with two interlocking eccentric bushings. The bushings enable the use of a conventional aerospace fastener in the joint without rework, like the transfer of hole patterns from the wing cover to a new replacement leading edge that is otherwise an industry standard. The holes in the leading edge are oversized to hold the eccentric bushings, with the inner one providing a hole fitted to the fastener type. Both bushings have the same eccentricity, enabling a hole-to-hole assembly in a radius ranging from zero to two times the eccentricity, depending on their relative angular placement. Depending on the initial position, a sequence

of angular progression for both eccentric bushings can be determined which generates a purely vertical movement between the joined parts. This enables the facilitation of a safe contact between the leading edge and wing cover. The leading edge and the attachment concept was designed in detail in a wing FE model with aerodynamic and thermal loads in cruise flight, different temperature on-ground and manoeuvre load cases. FIGURE 2 shows the leading edge final design with the attachment concept details enlarged.

For the production of the leading edge, a one-sided, three-part Ni36 steel mould is used in a prepreg autoclave process. The leading edge is produced in a one-shot process, including the addition of the steel foil erosion protection and the layers of the anti-ice system. A detailed account of the process development and production of the demonstrator leading edges is given by Buggisch [5]. Further details on the leading edge concept and the design process can be found in [4], [6], [7].

### 3. TEST STAND DESIGN AND GROUND BASED DEMONSTRATOR

#### 3.1. Test Stand Design

The main challenge of the test stand design is to replicate realistic ground based demonstrator surface deformations. In real life aircraft applications, the wing is loaded in flight by aerodynamic loads attacking at each surface increment while mass loads of the structure are equally dispersed throughout the structure. To replicate the on-ground free cantilevered wing and cruise flight deformations created by continuous loads in a laboratory environment using discrete load introduction, a special test stand design approach is needed.

For the upper wing surface shape, and especially the leading edge joint area, is in scope of the tests, a lower wing cover is not considered in the ground based demonstrator. The deformation of a complete wing box would have required far greater loads for the same outcome. The upper wing cover used is a pre-existing component, designed and built in a German national funded project. The wing cover includes integral stringers and ribcaps to support natural laminar flow. Design and production are documented by Ueckert [8] and Huehne [9].

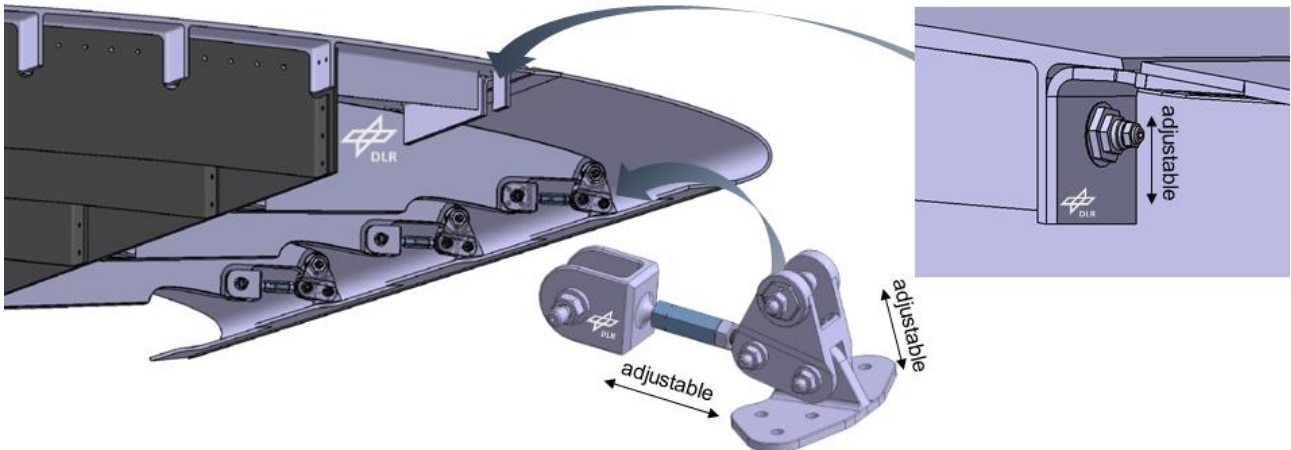


FIGURE 2. View of the GBD CAD with the final design of the pendulum strut.

Along the wing cover and leading edge, the GBD includes a front spar, five wing box ribs behind the front spar and eight forward wing ribs, of which two are designed as end ribs to support the leading edge profile. The forward wing ribs are not optimized as part of the test stand design process. Their simplified design is taken from the full wing FE design stage. Wing box ribs and front spar are part of the test stand optimization process. Their mechanical properties are tailored to support the translation of actuator loads to desired wing surface deformation. Inputs for the optimization process are the FE model of the wing

cover and leading edge and the surface target shapes taken from the FE design phase. A Python script governs the optimization, using the Mixed-Integer-Distributed-Ant-Colony-Optimization (MIDACO) algorithm [10] to iterate the parameters of the FE model. In order to mitigate the long runtime of each simulation, the Python library DASK [11] is utilized. It is a framework for distributing calculations to other workers, like different CPUs or in this application, over a network.

The initial optimization targeted the following optimization parameters:

- Thickness (function of material cured ply thickness and number of plies per fibre direction) of ribs and front spar
  - $(t_{p_1}: 0^\circ, t_{p_2}: 45^\circ, t_{p_3}: -45^\circ, t_{p_4}: 90^\circ)_s$ ,
  - $t$  between  $[1, 30]$ ,  $t \in \mathbb{Z}$
- Height of ribs and front spar
  - $h$  between  $[25\text{mm}, 200\text{mm}]$ ,  $h \in \mathbb{R}$
- Elongation of each actuator, modelled as thermal expansion
  - $\epsilon_{\text{therm}}$  between  $[-1, 1]$ ,  $\epsilon_{\text{therm}} \in \mathbb{R}$
- Action direction of each actuator, defined by two angles in the model coordinate system
  - $\alpha_1, \alpha_2$  between  $[-45^\circ, 45^\circ]$ ,  $\alpha \in \mathbb{R}$

The optimization function is the minimization of the deviation of surface deformation achieved by the optimization run and the predefined deformation.

This deviation was assessed at 21 predefined nodes, each in the middle of a skin section of the wing upper cover defined by the surrounding stringers and ribcaps (FIG. 4). The strength of all composite components was assessed as an additional constraint. A maximum allowable first principle strain of 0.0035 is used.

Five ribs were defined according to the positions given by the ribcaps of the wing cover to be used in the demonstrator structure. The attachment position of actuators to be used for load introduction into the ribs, their elongation and action direction were to be varied. To enable a deformation of the structure not only in span, but also chordwise direction, 15 actuators, 3 at each rib, were used in the first optimization runs.

To reduce the necessary elongations of the actuators and actuator force, the neural plane for the demonstrator was initially set to be the middle rib of the ground based demonstrator.

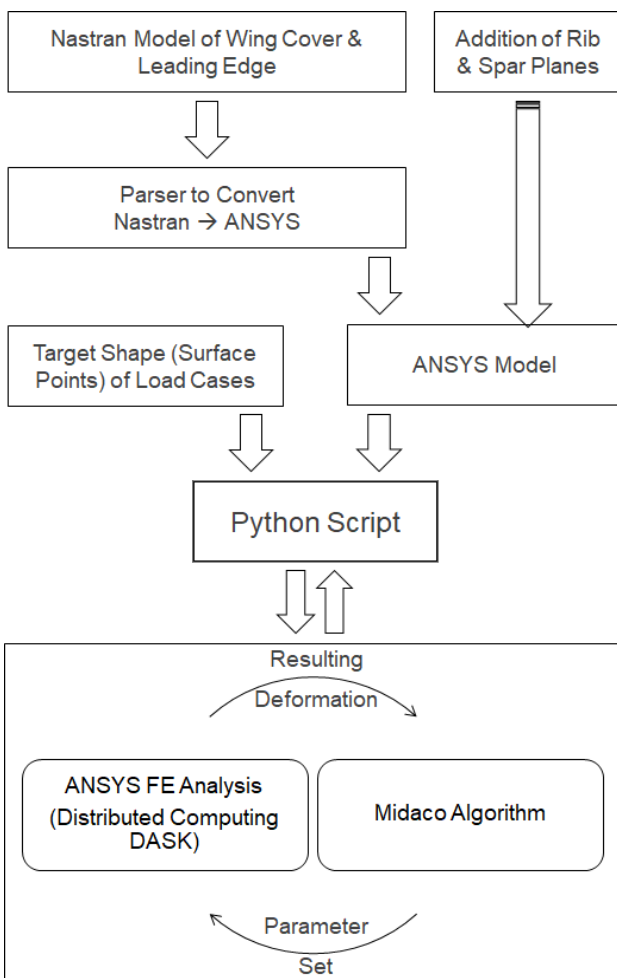


FIGURE 3. Optimization procedure flow chart.

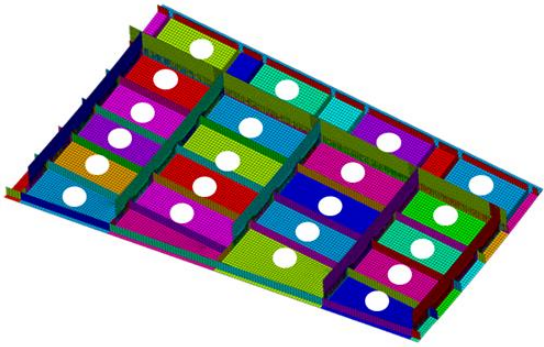


FIGURE 4. Target nodes for the optimization function on the wing cover (with ribs and spar, view from below).

The end-to-end relative displacements of the demonstrator would stay the same, just not in the intuitive “tip is higher than root” orientation, but with both inner end and outer end of the wing section being deformed upward. This approach was pursued in the design phase of the composite ribs and spars and led to the design freeze and manufacturing of these components. As a result of issues with the minimum displacement capability of the required electro-mechanical actuators encountered in the test stand procurement phase, an additional optimization loop was initiated. Shifting the neutral plane to the inner rib, now acting as a fixed bearing. Actuators were placed under the middle and outer rib in a vertical setup and one actuator was used to counter lateral movement parallel to the ground by non-vertical connection to the front spar. Actuator elongations were then again optimized, resulting in the final layout of the test stand replicating a surface deformation in the intuitive wing orientation. In the final configuration, the test stand includes 6 actuators, each capable of applying 5kn of force. Figure 6 shows the final design. The actuator control parameter is their elongation, with force measured to ensure safe operation and to provide additional information. A slotted table provides a stable platform for the test stand.

For the on-ground deformation case, 1.77mm deviation over all points used was achieved as an optimum. For cruise deformation (FIG. 5), 14.7mm deviation over all points used was achieved.

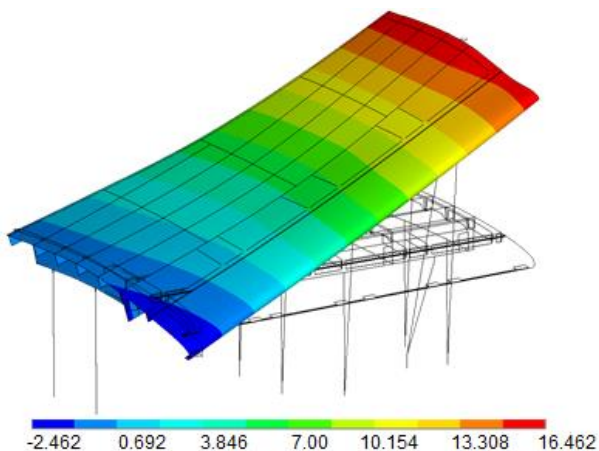


FIGURE 5. Surface deformation for the cruise load case, result of optimization run (deformation exaggerated).

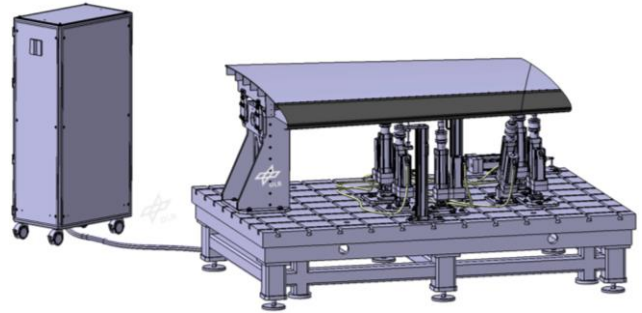


FIGURE 6. Rendering of the GBD integrated in the test stand's final configuration.

### 3.2. Demonstrator Integration

The assembly of wing cover, box ribs and front spar was done using an actuated, robot supported jig holding the wing cover and enabling its manipulation to match its nominal shape [12]. Ribs and spar were joined to the wing cover with conventional aerospace fasteners.

The test stand was delivered as a subcontracted module and integrated with the wing cover and rib assembly via machined fittings. Installation of the forward wing ribs was done with specialized assembly jigs for each rib, with the integral ribcaps of the wing cover used as spanwise reference. After joining the ribs to the ribcaps, a fitting was added to connect each rib with the front spar.

The leading edge installation itself was done by loosely inserting the bolts at the end ribs at first to secure the leading edge, followed by the connection of the rods between leading edge and ribs. The eccentric bushings and fasteners at the leading edge-to-upper cover joint were then placed, the fasteners tightened to a level where no axial movement takes place anymore. The eccentric bushings are adjusted beginning in the middle, moving on in inboard and outboard direction in an alternating manner. The adjustment process to bring leading edge landing and wing cover overhang to a safe is assisted by a light-gap method. An LED strip's glow is observed through the gap between the loosely fitted parts and the eccentric bushings are adjusted to produce an upward relative movement of the leading edge until the glow is no longer visible. Afterwards, the fasteners are properly tightened.



FIGURE 7. Full GBD with leading edge, integrated in the test stand (partial view).

### 3.3. Test Program and Initial Results

As described above, the test stand allows to deform the GBD structure to cruise and on-ground surface deformation states. With addition of the undeformed state, thus, three shapes of the structure exist for measuring. Only the end states are to be addressed, no transient or dynamic states will be in scope of the test campaign. Two leading edges are available for the installation and interchange trials. TAB 1 summarizes all planned installation runs of the leading edges, 3D measurements and the scope w.r.t. the analysis of the step between leading edge and wing cover. Each deformation state is measured with a GOM Atos 3D measuring system. Until the writing of this paper, the first installation of a leading edge (LE #1) has been conducted in the neutral deformation state. The installation of the leading edge and the 3D measurement of the GBD surface in all three deformation states were completed within a working day, with the installation done by two technicians. More

detailed time information will be gathered in the interchange trials, documenting the time to remove leading edge #1 and installing leading edge #2. FIG. 8 shows a comparison of the cruise and on-ground deformation cases of the GBD with LE #1 installed with the neutral deformation case as a reference. The amplitudes and shape of the deformations match the expectations and are suitable to support the intended investigations.

The analysis of the step height between leading edge and wing cover for all deformation cases of the first installation of LE #1 is still ongoing. A first approach using exported surface sections in a manual process delivered promising results. With sections analyzed every 30mm in spanwise direction, for all cases the measured step height was within the required NLF tolerance band. However, the application of an automated approach to the step height analysis is desirable and is pursued for a comprehensive analysis of all installation cases.

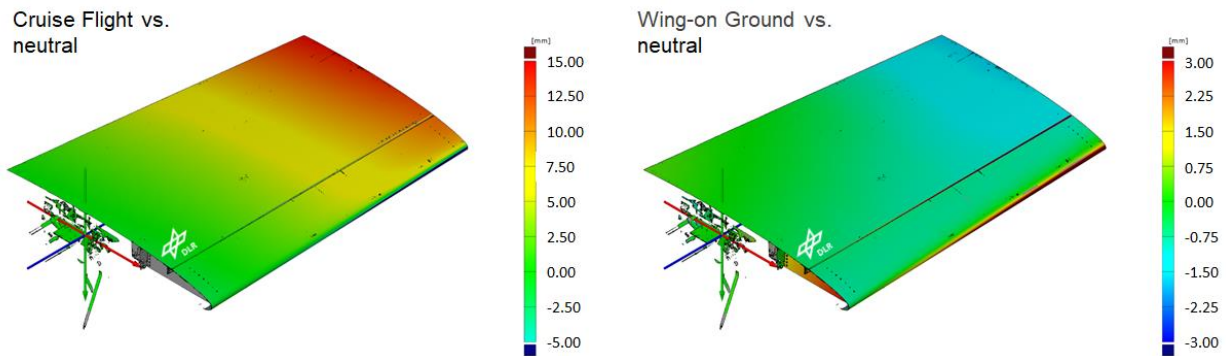


FIGURE 8. Global deformation of the GBD surface, first installation of LE#1.

Installation state vs. measured state	LE#1 first installation	LE#1 second installation	LE#2 first installation	LE#2 second installation	Scope of test series
Neutral → neutral	x	x	x		Repeatability of installation; identification of pot. differences between LE1 and LE2; general validation of interchangeability
Neutral → on-ground	x	x	x		Repeatability of deformation behavior for different installations
Neutral → cruise	x	x	x		Repeatability of deformation behavior for different installations; Validation of NLF attachment concept
On-ground → on-ground				x	Validation of interchangeability under operational conditions
On-ground → neutral				x	Reversibility of deformations
On-ground → cruise				x	Influence of first installation state on cruise deformation

TAB 1. Planned installation and interchange trials.

#### 4. SUMMARY AND OUTLOOK

In the Clean Sky 2 NACOR project, a multi-material, multi-functional composite leading edge was developed for an NLF wing. To validate the design and to demonstrate operational applicability of the leading edge and its specialized NLF compatible attachment concept, a test stand was designed. A multi-parameter optimization process was developed to design a test stand architecture that enables the deformation of a leading edge section installed to a wing cover to desired surface deformations. A test stand was designed using this process based on the on-ground and cruise flight surface deformation cases taken from the wing FE model created in the leading edge design process. Two leading edges were built and assembled to a wing section ground based demonstrator and integrated with the test stand.

Deformation trials validated the test stand design. Further trials will focus on the leading edge: To demonstrate applicability of the NLF leading edge design and attachment concept for airline operations, interchange trials with the two leading edges will be conducted, including installation of a replacement leading edge under a free-cantilevered wing-on-ground deformation. The step between leading edge and wing cover will be assessed regarding its compatibility with NLF requirements.

#### ACKNOWLEDGEMENTS

This project has received funding from the Clean Sky 2 Joint Undertaking under the European Union's Horizon 2020 research and innovation programme under grant agreement No CS2-AIR- GAM- 2014-2015-01

#### AUTHOR STATEMENT

**O. Steffen:** Conceptualization, Investigation, Writing, Supervision. **M. Buggisch:** Investigation. **J. Kosmann:** Investigation, Formal Analysis. **E. Kappel:** Investigation. **H. Köke:** Methodology (test stand optimization), Software (test stand optimization). **C. Hühne:** Funding acquisition.

#### LITERATURE

- [1] Schrauf, G., "Status and perspective of laminar flow", The Aeronautical Journal, Volume 109, Issue 1102, pp. 639-644, December 2005, P.639, <https://doi.org/10.1017/S00019240000097X>.
- [2] Hansen, H., Schlipf, B., „Laminarität für zukünftige Verkehrsflugzeuge – Ueberblick, Anforderungen und Status“, Wissenschaftstag des Instituts für Faserverbundleichtbau und Adaptronik, DLR, October 2015, Brunswick, Germany.
- [3] Holmes, B., Obara, C., Martin, G., and Domack, C., "Manufacturing Tolerances for Natural Laminar Flow Airframe Surfaces," SAE Technical Paper 850863, 1985, <https://doi.org/10.4271/850863>.
- [4] Steffen, O. Ueckert, C., Kappel, E., Bach, T. Huehne, C., "A multi-material, multi-functional leading edge for the laminar flow wing", 27th SICOMP Conference, May 30<sup>th</sup> -31<sup>st</sup>, 2016, Linköping, Sweden.

- [5] M. Buggisch, Entwicklung eines Fertigungsprozesses für eine laminare Flügelvorderkante, Deutscher Luft- und Raumfahrtkongress, Bremen, 2021, Germany.
- [6] C. Hühne, C. Ückert, O. Steffen, Multifunktionale Flügelvorderkante in Multimaterialbauweise, Lightweight Des 9, 28–33 (2016), <https://doi.org/10.1007/s35725-015-0065-6>.
- [7] O. Steffen, M. Buggisch, E. Kappel, H. Köke, P. Meyer, C. Hühne, Flight Testing on Ground – The Laminar Wing Leading Edge Ground Based Demonstrator, Deutscher Luft- und Raumfahrtkongress, Darmstadt, 2019, Germany.
- [8] C. Ueckert, T. Bach, E. Kappel, L. Heinrich, O. Steffen, CFRP Upper Wing Cover for Natural Laminar Flow. In: 27th SICOMP Conference on Manufacturing & Design of Composites. Sicomp 27th, 30.-31. Mai 2016, Linköping, Schweden.
- [9] Hühne, C., Ückert, C. & Steffen, O. Entwicklung einer laminaren Flügelschale, Lightweight Des 8, 32–37 (2015) <https://doi.org/10.1007/s35725-015-0054-9>.
- [10] <http://www.midaco-solver.com/> .
- [11] <http://docs.dask.org/en/latest/>
- [12] M. Bock, M. Kleineberg, Assembly 4.0 - Flexibly Picked Up, Precisely Mounted, SAE Int. J. Adv. & Curr. Prac. in Mobility 1(2) 352-356, 2019, <https://doi.org/10.4271/2019-01-1355>.

#### CORRESPONDING AUTHOR

Olaf Steffen, [olaf.steffen@dlr.de](mailto:olaf.steffen@dlr.de).